Journal of Systems Engineering and Electronics
Vol. 28, No. 6, December 2017, pp.1193 – 1202

EXCLUSIVELY AVAILABLE VIA
IEEE Xplore® DIGITAL LIBRARY

Improved bias proportional navigation with multiple constraints for guide ammunition

Wei Pang*, Xiaofang Xie, and Tao Sun

Department of Ordnance Science and Technology, Naval Aeronautical and Astronautical University, Yantai 264001, China

Abstract: According to the infrared guidance ammunition (GA) attacking non-maneuvering targets on the ground or sea level, an improved bias proportional navigation (IBPN) is put forward, which can meet the constraints of the impact angle and the angle of attack (AOA). The motion equations and the collision triangle for the GA and the target are established in the two-dimensional plane. In accordance with the collision triangle, the integral value of the bias term is solved and BPN is designed on the basis of the relative velocity. To ensure the new method can be solved, closed-loop equation of the IBPN is deduced. Considering the limitation of the AOA and the seeker angle, a four-phase IBPN is improved by setting different phases of the bias term. At the same time, the guidance law will make the impact angle achieve the desired angle and the normal acceleration also converges to zero. The simulation results show that the improved guidance law can be applied to various flight tasks and has great potential for engineering applications.

Keywords: improved proportional navigation, impact angle, bias term, look angle, normal acceleration.

DOI: 10.21629/JSEE.2017.06.17

1. Introduction

In recent years, in order to maximize the warhead effect of anti-ship or anti-tank weapons and improve the damage probability, many advance guidance laws with terminal impact angle constraints and other constraints have been widely studied in the missile guidance literature. In [1], Kim and Grider were the first to improve the impact angle constrained guidance law for the reentry vehicles, which turn the impact angle problems into the linear system. An accuracy of time-to-go estimation was improved for the energy-optimal impact control law that was derived from the linear quadratic guidance law in [2,3]. In order to reduce the terminal normal acceleration and eliminate the gravity disturbance, an extended optimal guidance law with terminal constraints of miss distance and impact angle was proposed by Ran [4]. In consideration of the characteristic for the missile overload, the trajectory shaping guidance law with impact angle constraints and terminal position was derived by the linear quadratic optimal control theory in [5]. Considering the reason that a constant gravity over compensation, which is widely used in the proportional navigation (PN), may lead to a larger terminal angle of attack (AOA) on the impact, a proportional navigation guidance law with variable gravity compensation coefficient was proposed in [6]. A novel guidance law named retro-proportional navigation was put forward in [7], which is designed to intercept targets of higher speed than the interceptor. It uses the negative navigation constant and intercepts the target at the farther collision triangle. Because the classical PN cannot realize the whole angles constraints interception of the target under the minimum guidance proportional coefficient, the two-stage PN composed of missile attitude adjustment state and target interception stage was proposed [8]. Considering the field-of-view (FOV) angle, acceleration constraints and the impact angle, Huang [9] proposed a three-phase bias-shaping method for the biased proportional guidance. In order to attack the top of a target at a large terminal angle, based on the optimal guidance law, Xie [10] proposed a guidance law with an amendment part. The part works if the view angle exceeds the predefined value. Considering the reason of the classical proportional navigation guidance cannot cover the range of impact angles $[0-\pi]$ against stationary targets when the navigation constant is $N < 2$, the two-stage proportional navigation guidance (PNG) law is proposed: in the first stage, the missile follows the orientation trajectory until the flight path angle (FPA) meets a certain value and then switches to the classical PN [11]; In [12], a two-phase bias pure proportional navigation (BPPN) guidance law was proposed. In the first phase, the missile follows the BPPN with a constant value

Manuscript received April 05, 2016.
*Corresponding author.
This work was supported by the China Postdoctoral Science Foundation (2013T60923).

bias term until the integral bias term reaches a certain value, and then removes the bias term into pure proportional navigation (PPN) in the second phase. Based on the two-phase bias proportional navigation (BPN) guidance scheme, Kim [13] first proposed a bias-shaping method to overcome the limitation of missile acceleration capability and high look angle's constraint, which may cause the seeker lock-on failure for the target.

However, these above guidance schemes have some drawbacks:

(i) As these guidance laws are established by the guidance ammunition (GA) constant velocity, they may be not suitable for the GA. Because the GA's velocity changing with the distance between the missile and the target, these methods may cause the FOV angle to exceed the predefined value, what's more, those may lead to excessive end acceleration.

(ii) Without considering the limitation of the look angle, when the GA reaches the target, it may exceed the seeker's FOV that will miss the target and result in the failure of tracking the target.

(iii) For the non-maneuvers target, the GA may produce a bounce in the end collision when the normal acceleration is bigger.

In this paper, we propose an improved bias proportion navigation (IBPN) based on PN [13] to overcome these defects, which can achieve both the terminal impact angle constraints and look angle limitation to maintain the seeker lock on the non-maneuvering targets, at the same time, the normal acceleration of the GA is in the limitation. Nonlinear dynamic system equations for the GA are established and the bias term of IBPN is derived for the non-maneuvering targets. With the limitation of the look angle and AOA, different bias terms are designed for the guidance to ensure the missile attack the targets with a little overload and large impact angle. The simulation results show that IBPN features in three characteristics. Firstly, aerodynamic characteristics are considered in the proposed guidance law and the AOA is taken as the control value. The simulation results by the imposed method accord with the actual situation. Secondly, it has strong adaptability to non-maneuvering targets with different velocities. Thirdly, the guidance command is relatively simple and it can be easily realized by the AOA control system.

2. Kinematics equations of the GA

In the first place, we must establish the kinematics equations of the GA to design the guidance law. In this paper, the guidance law is designed in the planar scenario and the influence of the earth's rotation is neglected, so the kinematics model of the GA is carried out in the vertical plane as follows:

$$\begin{cases} \dot{x} = v_M \cos\theta_M \\ \dot{y} = v_M \sin\theta_M \\ \dot{v}_M = -\dfrac{\rho v_M^2 s C_D}{2m} - g\sin\theta_M \\ \dot{\theta}_M = \dfrac{\rho v_M s C_L}{2m} - \dfrac{g\cos\theta_M}{v_M} \end{cases} \tag{1}$$

where x is the horizontal position and y is the altitude of the GA in the ballistic coordinates. v_M and θ_M denote the velocity and the FPA of the GA, respectively. m is the mass and s is the reference area of the GA, respectively. ρ is the air density. C_D and C_L are the drag and lift coefficients dependent on the AOA α and Mach number Ma.

Under the assumptions that α is small and the velocity of GA is less than the sound velocity. The drag coefficients and the lift coefficients can be approximated as the function for α and Ma, respectively.

$$\begin{cases} C_D(\alpha, Ma) = cd_0\alpha - cd_1 Ma + cd_2 \\ C_L(\alpha, Ma) = cl_1\alpha \end{cases} \tag{2}$$

where cd_0, cd_1, cd_2, cl_1 are the coefficients those fitting the AOA on different Ma [12], respectively.

3. IBPN for impact angle constraints and AOA constraints

3.1 Framework of the IBPN

In this section, the relationship of the GA with the target in the vertical plane is established, shown in Fig. 1.

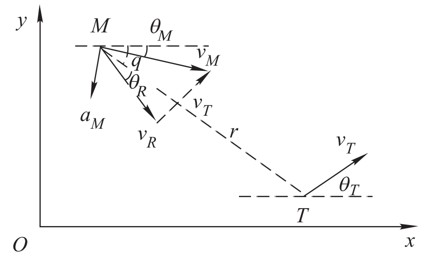

Fig. 1 Engagement geometry

In Fig. 1, a_M is the acceleration of the GA and q is the line-of-sight (LOS) angle; v_T and θ_T denote the velocity and the FPA of the target, respectively. v_R and θ_R denote the relative velocity and the relative FPA, respectively. In this paper, we assume the positive angle is the counterclockwise and the look-angle is the angle between the longitudinal axis and the LOS. Under the assumption that α is small, the look angle ψ can be represented as

$$\psi = \theta_M - q. \tag{3}$$

Based on the traditional PN, the IBPN is the relative FPA that adds the bias term [15]. Thus the FPA rate must obey

$$\dot{\theta}_R = N\dot{q} + b \tag{4}$$

where N is a constant that represents the navigation gain, b is the bias term, and

$$\theta_R = \arctan\left[\frac{(v_M \sin\theta_M - v_T \sin\theta_T)}{(v_M \cos\theta_M - v_T \cos\theta_T)}\right]. \tag{5}$$

Compared with the traditional BPN, (4) on the left is the relative FPA rate, so it is called the IBPN. However, $a_M = v_M\dot{\theta}_M$. By introducing the bias term b, the trajectory of GA is changed to satisfy certain constraint conditions.

3.2 Solution to the IBPN

Fig. 1 shows the relationship between the target and the GA. Here, we suppose that the target's velocity is invariable, and the nonlinear differential equation of the engagement can be written as

$$\begin{cases} v_R \cos\theta_R = v_M \cos\theta_M - v_T \cos\theta_T \\ v_R \sin\theta_R = v_M \sin\theta_M - v_T \sin\theta_T \end{cases}. \tag{6}$$

As the velocity of the target keeps constant, the derivative of (6) is

$$\begin{cases} \dot{v}_R \cos\theta_R - v_R \sin\theta_R\dot{\theta}_R = \dot{v}_M \cos\theta_M - v_M \sin\theta_M\dot{\theta}_M \\ \dot{v}_R \sin\theta_R + v_R \cos\theta_R\dot{\theta}_R = \dot{v}_M \sin\theta_M - v_M \cos\theta_M\dot{\theta}_M \end{cases}. \tag{7}$$

Using transformation of the trigonometric function, (7) turns into

$$\begin{cases} a_{M_x} = v_M\dot{\theta}_M = v_R\dot{\theta}_R \cos(\theta_R - \theta_M) + \dot{v}_R \sin(\theta_R - \theta_M) \\ a_{M_y} = \dot{v}_M = -v_R\dot{\theta}_R \sin(\theta_R - \theta_M) + \dot{v}_R \cos(\theta_R - \theta_M) \end{cases} \tag{8}$$

where a_{M_x} and a_{M_y} denote the normal acceleration and tangential acceleration, respectively. Conveniently, we set $a_M = a_{M_x}$ in this paper. In any case, (7) and (8) are correct as the geometry relation between the GA and the target derives them. If we expect an ideal impact angle, it will form a collision triangle before the GA attacks the target, as shown in Fig. 2.

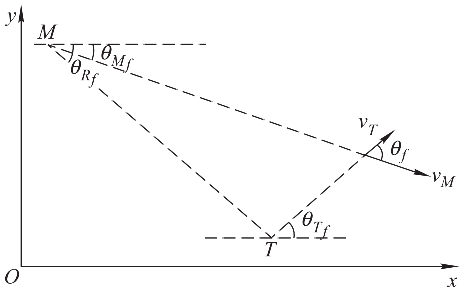

Fig. 2 Collision triangle

In Fig. 2, the subscript f denotes the terminal time, θ_f is a desired impact angle, which is defined by the difference between the FPA of the GA and the target.

$$\theta_f = \theta_{M_f} - \theta_{T_f} \tag{9}$$

Due to $v_M > v_T$, θ_{R_f} can be written as

$$\theta_{R_f} = \theta_T + \theta_f + \arcsin\left(\sin\theta_f \frac{v_T}{v_{R_f}}\right). \tag{10}$$

From (10), we can get $\theta_{R_f} = \theta_{M_f}$ when the target is stationary. If the impact relative velocity satisfies (10), the GA will attack the target at a desired impact angle.

3.3 Integration of the bias term

Integrating (4) with the initial conditions θ_{M_0} and q_0 yields

$$\theta_R(t) = \theta_{R_0} + N[q(t) - q_0] + \int_0^t b\mathrm{d}t. \tag{11}$$

If the GA successfully intercepts the target with a desired impact angle defined by θ_f,

$$q(t_f) = \theta_{R_f}. \tag{12}$$

Substituting (12) into (11) yields

$$\int_0^{t_f} b\mathrm{d}t = \theta_{R_f} - \theta_{R_0} - N[\theta_{R_f} - q_0]. \tag{13}$$

Set

$$Bref = \theta_{R_f} - \theta_{R_0} - N[\theta_{R_f} - q_0]. \tag{14}$$

Substituting (14) into (13) yields

$$\int_0^{t_f} b\mathrm{d}t = Bref. \tag{15}$$

Substituting (10) into (14) yields

$$Bref = \theta_{R_f} - \theta_{R_0} - N\left[\theta_{T_f} + \theta_f + \arcsin\left(\sin\theta_f \frac{v_T}{v_{R_f}}\right) - q_0\right]. \tag{16}$$

If the GA attacks the stationary target or non-stationary non-maneuvering targets, the integration of the bias term is decided by θ_{M_f}, θ_{M_0}, θ_{T_f}, θ_f, v_T, v_{R_f}, q_0 and N. Only v_{R_f} is unknown. v_{R_f} can be estimated according to the initial height and the initial velocity v_{M_0} of the GA.

Equation (16) only gets the integration of the bias term, it must acquire the bias term in the guidance law.

3.4 Closed-loop solution to the guidance

As Fig. 1 shows, the relationship of the relative distance r and LOS rate is as follows:

$$\begin{cases} \dot{r} = -v_M \cos(\theta_M - q) + v_T \cos(q - \theta_T) \\ r\dot{q} = -v_M \sin(\theta_M - q) - v_T \sin(q - \theta_T) \end{cases}. \tag{17}$$

Define the equation

$$\psi_R = \theta_R - q. \tag{18}$$

Combining (18) and substituting (6) into (17) yield

$$\begin{cases} \dot{r} = -v_R \cos\psi_R \\ r\dot{q} = -v_R \sin\psi_R \end{cases}. \tag{19}$$

Differentiating (18) with respect time, using (19) and (4), we can get

$$\begin{cases} \dot{r} = -v_R \cos\psi_R \\ \dot{\psi}_R = -(N-1)v_R \dfrac{\sin\psi_R}{r} + b \end{cases}. \tag{20}$$

Introducing $\chi = |\kappa| r$, where $\kappa = \dfrac{b}{v_R}$ is a constant and $\mathrm{d}\tau = |b|\mathrm{d}t$. Hence (20) turns into

$$\begin{cases} \dfrac{\mathrm{d}\chi}{\mathrm{d}\tau} = -\cos\psi_R & \text{(21a)} \\ \dfrac{\mathrm{d}\psi_R}{\mathrm{d}\tau} = -(N-1)\dfrac{\sin\psi_R}{\chi} + \sigma & \text{(21b)} \end{cases}$$

where σ denotes the sign of the bias term b and its value is -1 or $+1$. Equation (21) is consistent with [13]. Due to $|\psi_R| < \pi$, the equilibrium point of nonlinear (21) is

$$\{\chi_e, \psi_{R,e}\} = \left\{\sigma(N-1), \frac{\pi}{2}\right\}$$

and

$$\{\chi_e, \psi_{R,e}\} = \left\{\sigma(1-N), -\frac{\pi}{2}\right\}.$$

Since $r \geqslant 0$ and $N > 1$, the first equilibrium point is $\{N > 1, \delta = 1\}$ and the second is $\delta = -1$.

Equation (21b) dividing (21a) yields

$$\frac{\mathrm{d}}{\mathrm{d}\chi}\sin\psi_R = (N-1)\frac{\sin\psi_R}{\chi} - \sigma. \tag{22}$$

When $N \neq 2$, the solution to (22) is

$$\sin\psi_R = c\chi^{N-1} + \frac{\sigma}{N-2}\chi. \tag{23}$$

When $N = 2$, the solution is as follows:

$$\sin\psi_R = \chi(\sigma \ln\chi + c). \tag{24}$$

Here, c is an integration constant. When $N \leqslant 2$, it may generate infinite guidance, so we only consider $N > 2$ in this paper. Erer points out that only c satisfies some conditions, the GA can attack the targets properly [12]. For details can be seen in [12]. Substituting $N = 3$ and $\sigma = 1$ into (24) yields the integration constant:

$$c_e = -\frac{1}{(N-1)^{N-1}(N-2)}. \tag{25}$$

When $\sigma = 1$ and $c > c_e, \chi < \chi_e$ or $c < c_e, \psi_R < \dfrac{\pi}{2}$ (when $\sigma = -1, c < c_e, \chi < \chi_e$ or $c < c_e, \psi_R > -\dfrac{\pi}{2}$), the trajectory of the GA is convergent [10].

From (20), (21), (23), we get

$$\frac{\mathrm{d}\theta_R}{\mathrm{d}\tau} = -cN\chi^{N-2} - \frac{2\sigma}{N-2}. \tag{26}$$

Combining (7) and (26), we get the conclusion that when the bias-term is not zero at the impact time, the normal acceleration is also not zero.

3.5 Bias term solution

From (1), we can get

$$\begin{cases} \dot{v}_M = -\dfrac{\rho v_M^2 s C_D}{2m} - g\sin\theta_M = a_{M_y} \\ v_M\dot{\theta}_M = \dfrac{\rho v_M s C_L}{2m} - \dfrac{g\cos\theta_M}{v_M} = a_M \end{cases}. \tag{27}$$

From (27) and (4), if the LOS rate and the bias term are known, it will get the executable guidance law. The home seeker can obtain the LOS rate and the bias term will be used as input for the control system, which will be solved for IBPN.

Using Erer's thought [12], the two-phase BPN is designed. Different from that in [12], which keeps a constant, the bias term b is a value changing with time. Next, we will talk about the solution of the bias term for the two phases.

In the first phase, using the IBPN until the integration of the bias term satisfies (13), then turn to the second phase and IBPN switches to PN without the bias term.

In order to ensure that the GA attacks the target, the initial b_0 must be a reasonable value. From (16), we get

$$b_0 = \frac{\theta_{M_f} - \theta_{M_0} - N\left[\theta_{T_f} + \theta_f + \arcsin\left(\sin\theta_f \dfrac{v_T}{v_{R_f}}\right) - q_0\right]}{r_0/v_{R,0}}. \tag{28}$$

Integrating (4) from (t, t_f), we get

$$\int_t^{t_f} b(\tau)\mathrm{d}\tau = Bref(t). \tag{29}$$

where

$$Bref(t) = \theta_{M_f} - \theta_M(t) - N\left[\theta_T(t) + \theta_f + \arcsin\left(\sin\theta_f \frac{v_T}{v_{R_f}}\right) - q(t)\right]. \tag{30}$$

When $\tau \in (t, t_f)$, $b(\tau) = b(t)$, the bias term is

$$b(t) = \frac{Bref(t)}{t_{go}} \tag{31}$$

where $t_{go} = t_f - t$ is the time-to-go. According to [14], we get the time-to-go estimation method for the IBPN guidance law.

$$t_{go} \approx \frac{r}{v_M}\left[1 + \frac{(q(t) - \theta_M)^2}{2(2N-1)} + \right.$$

$$\left.\frac{(\theta_1+N\theta_2)^2\times(-3\theta_2+\theta_1 N\theta_2)}{3(N+1)(2N-1)}\right] \tag{32}$$

where $\theta_1=\theta_M-\theta_f$ and $\theta_2=\theta_{M_f}-q(t)$.

The bias term b will change with $q(t)$, $\theta_M(t)$, $\theta_R(t)$ and v_M, which will has certain adaptability to the non-maneuvering target.

4. Considering the look angle and AOA

In the third section, we just introduce the solution to the bias term without considering the limitation of the AOA and the look angle. In this section, the IBPN with those constraints will be discussed for the non-maneuvering target.

The look angle of the GA must satisfy

$$|\psi(t)|\leqslant\psi_{\max} \tag{33}$$

where $\psi_{\max}$ is the maximum look angle of the GA. The IBPN without considering the look angle may cause the GA missing the target as the engagement progress, so the IBPN guidance law should be improved to satisfy the limitation of the look angle and AOA.

Through the two-phase IBPN, we design the four-phase IBPN guidance law as shown in Fig. 3 and Fig. 4. In the first phase, use the max AOA to increase the look angle and the bias term is as follows:

$$b_1(t)=f(u_{\max}). \tag{34}$$

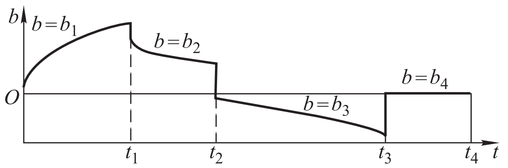

Fig. 3 Bias-term for the IBPN

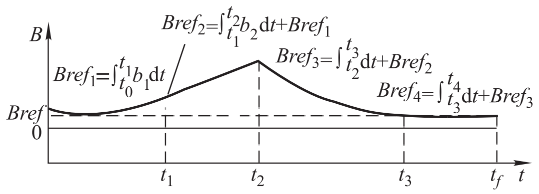

Fig. 4 Integration of bias-term for IBPN

When the look angle reaches the limitation, then turns to the second phase, the initial integration of the bias term is

$$B(t_1)=\int_0^{t_1} b_1(\tau)\mathrm{d}\tau. \tag{35}$$

In the second phase, the look angle should be kept the max value, and we get

$$\dot{\psi}=\dot{\theta}_M-\dot{q}=0. \tag{36}$$

Hence, the bias term is

$$b_2=(1-N)\dot{q}. \tag{37}$$

And the integration of the bias term is

$$B(t_2)=\int_{t_1}^{t_2} b_2(\tau)\mathrm{d}\tau. \tag{38}$$

In the third phase, we use the minimum AOA to reduce the bias term until it reaches a certain value, which is calculated by

$$b_3(t)=f(u_{\min}). \tag{39}$$

And the integration of the bias term is

$$B(t_3)=\int_{t_2}^{t_3} b_3(\tau)\mathrm{d}\tau. \tag{40}$$

The guidance law is

$$a_M=\frac{v_R(N\dot{q}+b_3(t))}{\cos(\theta_R-\theta_M)}. \tag{41}$$

Caution: In order to ensure forming a collision triangle before the GA attacks the target, the integration of the bias term must reach $Bref$ in the third phase.

In the fourth phase, because the integration of the bias term reaches the $Bref$ in the third phase, the bias term will be kept zero. Sometimes, the fourth phase is not necessary, but will not hurt. Whether the fourth phase exists or not, it is decided by t_2. If t_2 is a proper value, the integration of the bias term will be equal to $Bref$ in the end of the third phase when the interception happens.

In the fourth phase, if the integration of the bias term gets $Bref$, the bias term $b_4=0$ until the GA hits the target.

$$B(t)=\int_0^t b\mathrm{d}t=\int_0^{t_1} b_1\mathrm{d}t+\int_{t_1}^{t_2} b_2\mathrm{d}t+\int_{t_2}^{t_3} b_3\mathrm{d}t+\int_{t_3}^{t} b_4(\tau)\mathrm{d}\tau. \tag{42}$$

And the guidance law is

$$a_M=\frac{v_R N\dot{q}}{\cos(\theta_R-\theta_M)}. \tag{43}$$

And AOA could be calculated by (27). When the collision triangle is formed, the LOS rate will keep unchanged until the GA hits the target, in which $\dot{q}=0$. Due to $a_M=v_M\dot{\theta}_M$, the normal acceleration of the GA will become zero in the end.

5. Simulation results

To demonstrate the properties of the proposed guidance law in this paper, we assume the GA attacks non-maneuvering targets with the impact angle and control constraints. We use the BPN [15] and optimal guidance navigation (OGN) law [16] to compare with the IBPN. Four cases are considered in this paper.

5.1 For stationary targets

We consider the initial conditions of the GA as follows: $v_M = 250\ \mathrm{m/s}$ and the position $(x_M, y_M) = (0, 2\,000)$ m with $\theta_M = 0$, the position of the target $(x_T, y_T) = (3\ 000, 0)$ m. The impact angle $\theta_f = -60^\circ$ and $\psi_{\max} = 35^\circ$, simulations are terminated for the distance of the guided ammunition and the target $R < 0.1$ m or $R < v_R dt$, while $dt = 0.01$ s, which denotes the simulation step size. The guided ammunition using the IBPN has a limitation of attack angle $|\alpha| \leqslant 6^\circ$. The simulations of the scenario are presented in Fig. 5 and Table 1.

Fig. 5 presents the simulations results for the GA and the scenario by three methods. In the initial time, it will cost the kinetic energy to keep the GA at a high level and the look angle will reach the max limitation rapidly by the IBPN, then it will switch to the second phase. It can be seen clearly that the four phases by the IBPN are in Fig. 5(d) to Fig. 5(g).

Table 1 Index of three methods

Index	IBPN	BPN	OGN
Impact angle/(°)	–60.09	–60.27	–60.01
Miss distance/m	0.10	1.09	0.10
Attack angle (Max/Min)/(°)	–6/6	0/–4.36	3.94/–6
Look angle (Max/Min)/(°)	35/0	0.13/–33.69	0.97/–36.82
Flight time/s	15.81	15.2	16.12
Normal acceleration /(m/s^2)	–0.04	–19.34	4.89

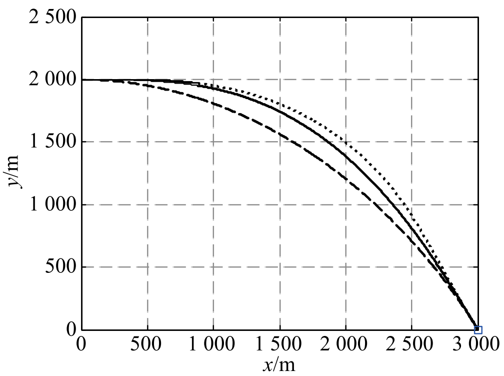

——: IBPN; – – –: BPN; ……: OGN; □ : TARGET.

(a) GA trajectory

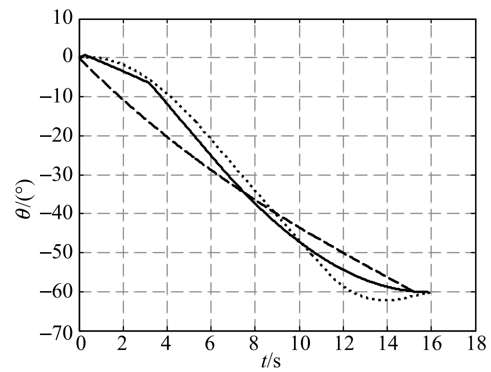

——: IBPN; – – –: BPN; ……: OGN.

(b) Impact angle

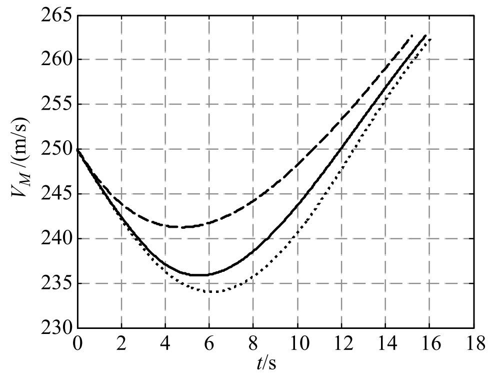

——: IBPN; – – –: BPN; ……: OGN.

(c) Velocity of the GA

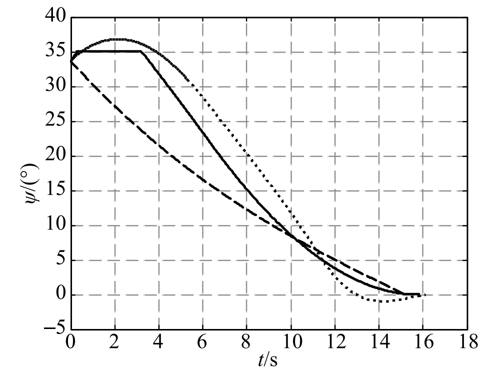

——: IBPN; – – –: BPN; ……: OGN.

(d) Look angle

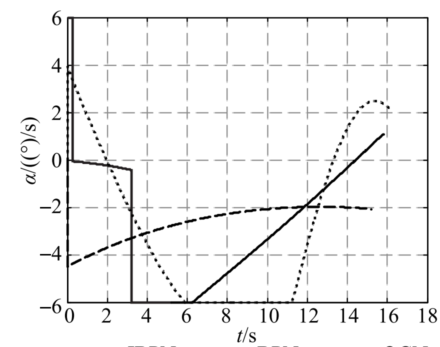

——: IBPN; – – –: BPN; ……: OGN.

(e) Attack angle

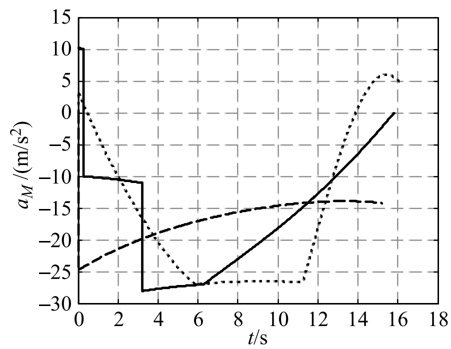

——: IBPN; – – –: BPN; ……: OGN.

(f) Normal acceleration

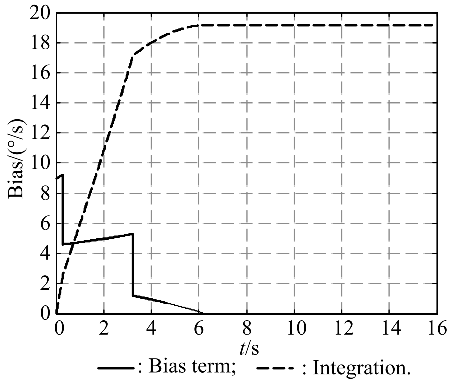

(g) Bias term and integration

Fig. 5 Results for the stationary target

Table 1 shows that the IBPN can satisfy the impact angle and AOA constraints as well as the look angle limitation, at the same time, the normal acceleration is smaller than other methods. The OGN has much little error angle, but the look angle will exceed $\psi_{\max}$, which will miss the target. The BPN will take less time but the normal acceleration is too big, which may cause the effect of bounce.

5.2 For non-maneuvering moving targets

In this section, the target is moving slowly (relative to the GA) without changing the directions. We consider the initial conditions of the GA as follows, $v_M = 250$ m/s and the position $(x_M, y_M) = (0, 2\ 000)$ m with $\theta_M = 0$, the initial position of the target $(x_M, y_M) = (4\ 000, 0)$ m and $v_T = 30$ m/s with $\theta_T = 10°$. Other conditions are the same to Section 5.1. The simulations of the scenario are presented in Fig. 6 and Table 2.

Fig. 6 presents the simulation results for the GA. The four phases are clearly indicated in Fig. 6(e) to Fig. 6(g). From Fig. 5(g) and Fig. 6(g), it can be seen that the integration of the bias term is different from the stationary targets. This is because the target is keep moving when the GA chases it. Table 2 shows that the impact angle error by the IBPN is about $0.1°$ and the normal acceleration is smaller than other methods.

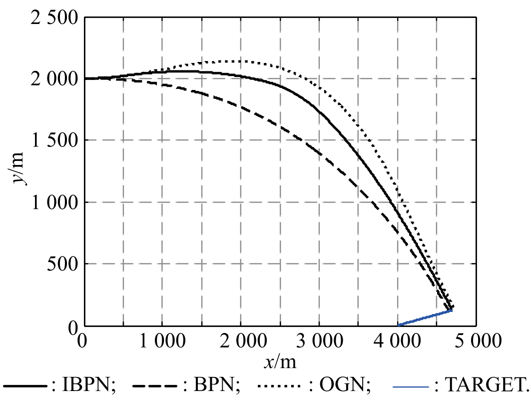

(a) GA trajectory

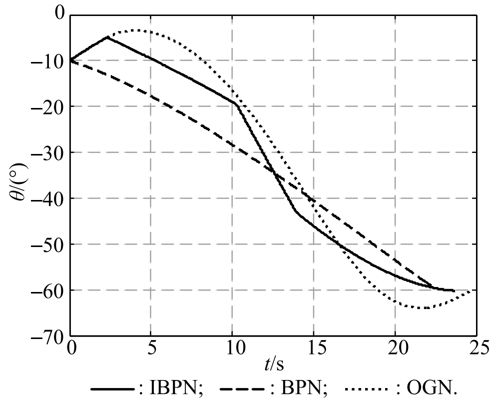

(b) Impact angle

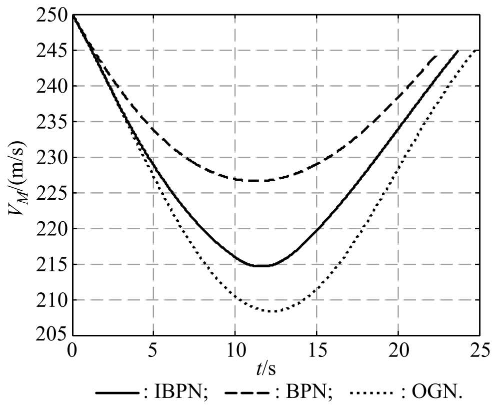

(c) Velocity of the GA

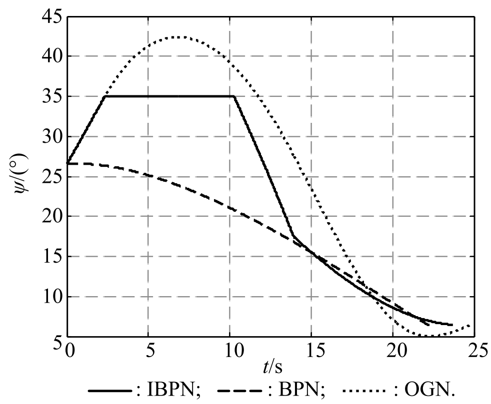

(d) Look angle

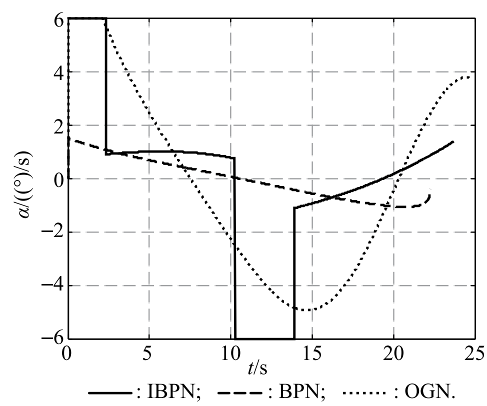

(e) Attack angle

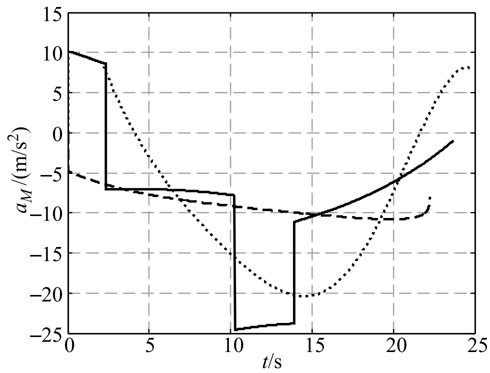

——: IBPN; – – –: BPN; ·······: OGN.

(f) Normal acceleration

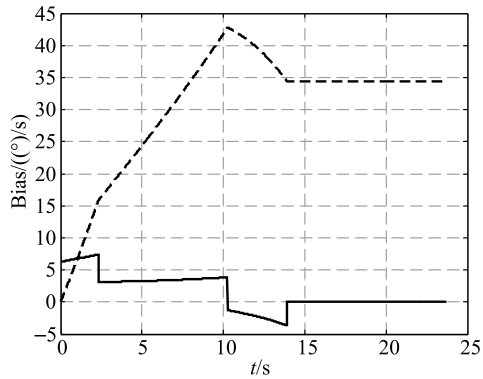

——: Bias term; – – –: Integration.

(g) Bias term and integration

Fig. 6 Results for the non-maneuvering moving target

Table 2 Index of three methods

Index	IBPN	BPN	OGN
Impact angle/(°)	–59.90	–59.02	–59.95
Miss distance/m	0.90	2.12	0.7
Attack angle (Max/Min)/(°)	6/–6	1.50/–1.07	6/–4.94
Look angle (Max/Min)/(°)	35/6.44	–6.42/–26.60	42.39/–5.06
Flight time/s	23.72	22.24	24.80
Normal acceleration /(m/s^2)	–0.24	–7.96	7.88

5.3 Miss distance with different target velocities

In this section, the miss distance with different target velocities is studied. The initial conditions are the same to Section 5.2 except the target's velocity, and the results are shown in Fig. 7 and Table 3.

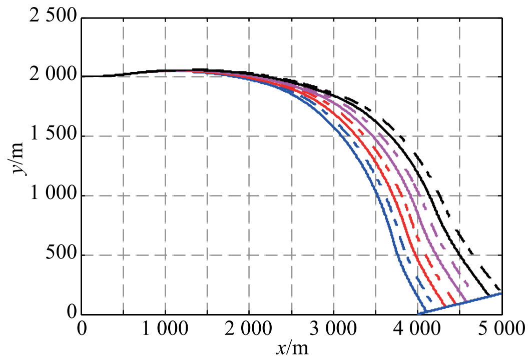

——: v_t=5 m/s; – – –: v_t=10 m/s; ——: v_t=15 m/s;
– – –: v_t=20 m/s; ——: v_t=25 m/s; – – –: v_t=30 m/s;
——: v_t=35 m/s; – – –: v_t=40 m/s.

Fig. 7 GA's trajectories with different target velocities

Table 3 Miss distance with different target velocities

Index	Target velocity/(m/s)							
Target velocity/(m/s)	5	10	15	20	25	30	35	40
Miss distance/m	0.26	0.35	0.46	0.5	0.7	0.9	1.0	1.15
Impact angle error/(°)	0.09	0.15	0.11	0.08	0.09	0.1	0.11	0.07

It can be concluded from Table 3, the impact angle error is very close to zero. The time-to-go estimation error increases with the target's velocity, that leads to the bias term generating error and increases the miss distance.

5.4 Monte Carlo simulations

In the previous cases, each simulation just focuses on one situation. In this section, many different situations are taken into consideration, such as the altitude error, the velocity error, the FPA, the aerodynamic modeling error and so on. In this section, we consider the initial state parameter perturbation as generated randomly uniform distribution and the range of dispersion is $\pm 20\%$. The aerodynamic model error ρ is set in the range of $\pm 10\%$. The Monte Carlo simulation for 500 times is shown in Fig. 8.

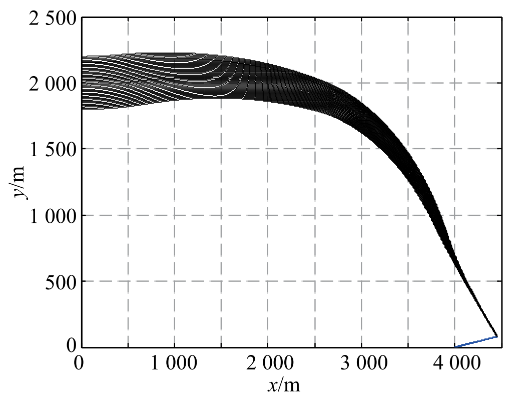

——: GA trajectory; ——: Target trajectory.

(a) GA's trajectories in (x,y) space

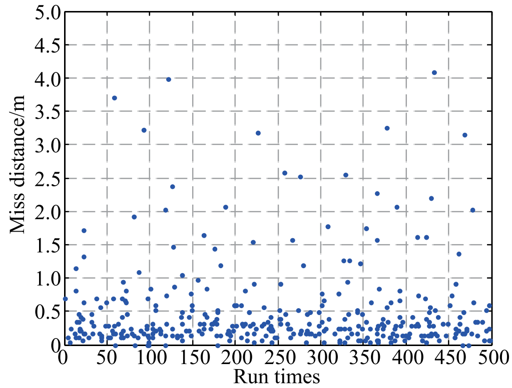

(b) Miss distance

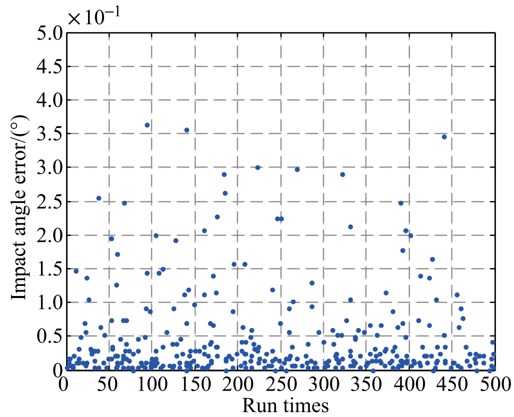

(c) Impact angle error

Fig. 8 Monte Carlo simulation results

Due to the initial perturbation in state parameters, we can see that the flight trajectories are significantly different from each other in Fig. 8(a). However, they all converge to one point at the end of the flight. Fig. 8(b) and Fig. 8(c) show that the miss distance and impact angle error are equally good under the severe conditions. For majority of the cases, the impact angle errors and the miss distances can meet the needs of combat. The average miss distance is 0.75 m and the average impact angle errors is 0.09°. The simulation results demonstrate that our method has better robustness and easy to realize.

6. Conclusions

An IBPN guidance law is designed for the no-maneuvering target, which is different from the traditional BPN. The relationship between the relative FPA rate and the LOS rate is established. A collision triangle is formed before the GA hits the target and the normal acceleration command is designed by the IBPN. Meanwhile, the conditions for stable trajectory of the IBPN are proved by the closed form solution.

Considering the constraints of the AOA and the look angle aiming at the no-maneuvering target, a four-phase bias term is designed. Conversion between different phases is decided by whether the required bias integral value reaches a certain value. In different phases, the bias term is designed by the time-to-go which has certain adaptability for different targets. The normal acceleration of the GA is less than other methods of normal acceleration when the target is hit.

The IBPN guidance law is quite robust to the initial conditions as well as the aerodynamic modeling error and the parameter perturbation.

The future work may include the extension of the IBPN to the three-dimensional guidance law and the trajectory shaping ability.

References

[1] M. Kim, K. V. Grider. Terminal guidance for impact attitude angle constrained flight trajectories. *IEEE Trans. on Aerospace and Electronic Systems*, 1973, 9(6): 852 – 859.

[2] C. Ryoo, H. Cho, M. Tahk. Optimal guidance laws with terminal impact angle constraint. *Journal of Guidance, Control, and Dynamics*, 2005, 28(4): 724 – 732.

[3] V. Shaferman, T. Shima. Linear quadratic guidance laws for imposing a terminal intercept angle. *Journal of Guidance, Control, and Dynamics*, 2008, 31(5): 1400 – 1412.

[4] R. Li, Q. L. Xia, Q. Q. Wen. Extended optimal guidance law with impact angle and acceleration constraints. *Journal of Systems Engineering and Electronics*, 2014, 25(5): 868 – 876.

[5] D. W. Liu, Q. L. Xia, T. Wu, et al. Trajectory shaping guidance law with terminal impact angle constraint. *Journal of Beijing Institute of Technology*, 2011, 20(3): 345 – 350.

[6] C. L. Yang, S. J. Tang, J. Shi. Proportional navigation guidance law with variable coefficient gravity compensation. *Journal of Beijing Institute of Technology*, 2009, 18(3): 304 – 308.

[7] H. M. Prasanna, D. Ghose. Retro-proportional navigation: a new guidance law for interception of high speed targets. *Journal of Guidance, Control, and Dynamics*, 2012, 35(2): 377 – 386.

[8] X. L. Chen, W. H. Hua. Ground target interception proportional navigation law with terminal constraints. *Journal of Ballistics*, 2010, 22(2): 15 – 18. (in Chinese)

[9] J. Huang, Y. A. Zhang, Y. X. Liu. A biased proportional guidance algorithm for moving target with impact angle and field of view constraints. *Journal of Astronautics*, 2016, 37(2): 195 – 202. (in Chinese)

[10] J. Xi, J. Yang, X. P. Zhu, et al. Guidance law design with impact angle and view angle constraints. *Electronics Optics & Control*, 2014, 21(9): 26 – 28, 89. (in Chinese)

[11] A. Ratnoo, D. Ghose. Impact angle constrained interception of stationary targets. *Journal of Guidance, Control and Dynamics*, 2008, 31(6): 1816 – 1821.

[12] K. S. Erer, O. Merttopcuoglu. Indirect impact-angle control against stationary targets using biased pure proportional navigation. *Journal of Guidance, Control, and Dynamics*, 2012, 35(2): 700 – 703.

[13] T. Kim, B. Park, M. Tahk. Bias-shaping method for biased proportional navigation with terminal angle constraint. *Journal of Guidance, Control, and Dynamics*, 2013, 36(6): 1810 – 1815.

[14] Y. Zhao, Y. Sheng, X. Liu. Sliding mode control based guidance law with impact angle constraint. *Chinese Journal of Aeronautics*, 2014, 27(1): 145 – 152.

[15] F. Gao, S. J. Tang, J. Shi, et al. A bias proportional navigation

guidance law based on terminal impact angle constraint. *Journal of Beijing Institute of Technology*, 2014, 34(3): 277 – 282. (in Chinese)

[16] M. Chao, R. S. Sun, C. J. Sun. Optimal guidance law to maximize terminal velocity for missiles with impact angle constraint. *Journal of Harbin Institute of Technology*, 2016, 23(2): 72 – 78.

Biographies

Wei Pang was born in 1987. He received his B.S. and M.S. degrees from Naval Aeronautical and Astronautical University (NAAU), Yantai, China, in 2011 and 2013 respectively. He is currently pursuing an Ph.D. degree at the Department of Ordnance Science and Technology of NAAU. His main research interests are modeling and simulation of weapon systems.
E-mail: metrix_yt@163.com

Xiaofang Xie was born in 1962. He is a professor and Ph.D. supervisor in the Department of Ordnance Science and Technology of NAAU. His current research interests are design of weapon systems and naval gun antimissile systems.
E-mail: xiexf@yahoo.com.cn

Tao Sun was born in 1980. He received his M.S. and Ph.D. degrees from NAAU, Yantai, China, in 2005 and 2009. His current research interest is intelligent design of weapon systems.
E-mail: mercury_tao@yahoo.com.cn